Fluorene–Carbazole Dendrimers: Synthesis, Thermal, Photophysical and Electroluminescent Device Properties

ARTICLE *in* ADVANCED FUNCTIONAL MATERIALS · DECEMBER 2010

Impact Factor: 11.81 · DOI: 10.1002/adfm.201001153

8 AUTHORS, INCLUDING:

Özlem Usluer
Necmettin Erbakan Üniversitesi
16 PUBLICATIONS **155** CITATIONS
SEE PROFILE

Daniel Ayuk Mbi Egbe
Johannes Kepler University Linz
116 PUBLICATIONS **2,036** CITATIONS
SEE PROFILE

Cem Tozlu
Karamanoglu Mehmetbey Üniversitesi
11 PUBLICATIONS **109** CITATIONS
SEE PROFILE

Alberto Montaigne Ramil
Johannes Kepler University Linz
29 PUBLICATIONS **557** CITATIONS
SEE PROFILE

Fluorene-Carbazole Dendrimers: Synthesis, Thermal, Photophysical and Electroluminescent Device Properties

By *Ozlem Usluer,* Serafettin Demic,* Daniel A. M. Egbe, Eckhard Birckner, Cem Tozlu, Almantas Pivrikas, Alberto Montaigne Ramil,* and *Niyazi Serdar Sariciftci*

Novel hole-transporting dendrimeric molecules containing dioctylfluorene, spirobi(fluorene) and spiro(cylododecane-fluorene) as the core unit and different numbers of carbazole and thiophene moieties as the peripheral groups are synthesized. All the dendrimers are characterized by ^{1}H NMR, ^{13}C NMR, FTIR, UV–vis, PL spectroscopy, and MALDI-TOF. They are thermally stable with high glass transition and decomposition temperatures and exhibit chemically reversible redox processes. They are used as the hole-transporting layer (HTL) material for multilayer organic light emitting diodes (OLEDs) with a low turn-on voltage of around 2.5 V and a bright green emission with a maximum luminance of around 25400 cd m^{-2}.

1. Introduction

Since the electroluminescence from small molecular organic materials was reported for the first time in 1987 by Tang and VanSlyke, organic light-emitting diodes (OLEDs) have attracted much attention and found their way into markets as displays.[1] With their advantages of low-power consumption, high contrast and high brightness, they have applications in full color flat panel displays.[2,3]

The general structure of OLEDs consists of a light emissive layer sandwiched in between two metal electrodes, one of which is transparent conducting electrode (**Figure 1**). Additional layers between the cathode and the emissive layer (electron transport layer, ETL) or between the anode and the emissive layer (hole transport layer, HTL) is used for high efficiency OLED devices. Recent studies revealed that organic multilayer structures typically enhance the performance of the devices by lowering the barrier for hole injection from the anode and by enabling control over the electron-hole recombination region, moving it from the organic/cathode interface, where the defect density is high, into the bulk. Hence, the layer deposited on the anode would generally be a good hole transport material (HTM), providing HTL. Similarly, the organic layer in contact with the cathode would be the optimized ETL.[4]

In general, high glass transition temperature (T_g) amorphous hole transport materials (AHTMs) are needed to have an efficient and stable OLED device. The most widely used HTLs, *N,N′*-bis(3-methylphenyl)-*N,N′*-diphenylbenzidine (TPD) and 4,4′-bis[*N*-(1-naphthyl)-*N*-phenyl-amino]biphenyl (NPB), offer many attractive properties such as high charge carrier mobility and ease of sublimation. They possess some disadvantages to be used in long-lifetime OLED devices such as their rather low T_g

[*] Dr. O. Usluer, Dr. S. Demic
Solar Energy Institute
Ege University,
35100, Bornova, Izmir (Turkey)
E-mail: ozlem.usluer@ege.edu.tr; serafettin.demic@ege.edu.tr
Dr. D. A. M. Egbe, Dr. A. Pivrikas, Dr. A. M. Ramil,
Prof. N. S. Sariciftci
Linz Institute for Organic Solar Cells (LIOS)
Physical Chemistry
Johannes Kepler University
Altenbergerstr. 69, A-4040 Linz (Austria)
Dr. E. Birckner
Institute of Physical Chemistry
Friedrich Schiller-University Jena
Lessingstrasse 10, 07743 Jena (Germany)
Dr. O. Usluer
Department of Chemistry
Art and Science Faculty
Mugla University
48000, Mugla (Turkey)
C. Tozlu
Department of Physics
Art and Science Faculty
Mugla University
48000-Mugla (Turkey)

DOI: 10.1002/adfm.201001153

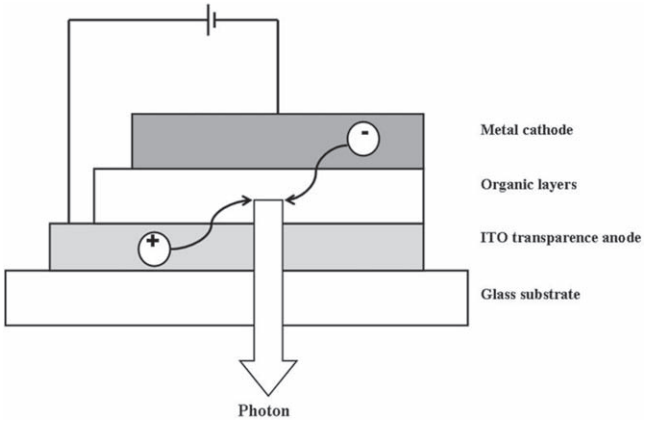

Figure 1. General structure of OLED device.

(~65 °C for TPD and ~100 °C for NPB), ease of crystallization and unsatisfactory morphological stability.[5,6] Recently, AHTMs with high T_g such as dendritic carbazole molecules with a fluorene core,[7,8] 1,4-bis(*N*-carbazolyl)benzene as a central unit and different numbers of diphenylamine moieties as the peripheral group,[9] 1,3,5-tris(2-(9-ethylcarbazolyl-3)ethylene)benzene,[10] 4,4′,4″-tri(*N*-dibenzocarbazolyl)triphenylamine[11] and monodisperse carbazole-based oligomers,[12] have been reported.

Carbazole molecules have been used as HTLs owing to their excellent hole-transporting capability, high charge carrier mobility, high thermal, morphological and photochemical stability.[13] It can easily be functionalized at its 3,6-, 2,7- or *N*-positions[14–16] and then covalently linked into polymeric systems, both as building blocks in the main chain[17] and pending groups in the side chain.[18]

It is known that fluorene derivatives are important materials for OLEDs because of their high quantum yield of photoluminescence (PL) and electroluminescence (EL) efficiencies and high thermal stabilities. Spiro-functionalization at the bridge position of fluorene (C-9) having a specific steric configuration has been attracting much attention as organic functional material in terms of its specific physical properties.[19]

In this paper, we report the synthesis, characterization and use of novel hole-transporting dendrimeric molecules containing octylfluorene, spirobi(fluorene) and spiro(cylododecanefluorene) core unit and different numbers of carbazole and thiophene moieties as the peripheral groups synthesized by divergent method. Their chemical structures were elucidated by ^{1}H NMR, ^{13}C NMR, FTIR and MALDI-TOF. Their photophysical, thermal and electrochemical properties were determined by UV–Vis and PL spectroscopies, cyclovoltammetry (CV), thermogravimetric analysis (TGA) and differential scanning calorimetry (DSC). Their hole-transporting properties were investigated by preparing multilayer OLED devices having the structure ITO/PEDOT:PSS/HTL(Dendrimer)/Alq_3/LiF:Al.

2. Results and Discussion

2.1. Synthesis

The synthetic routes of nine carbazole and thiophene based compounds are shown in **Schemes 1** to **3**. Coupling of 2,7-dibromo-9,9-dioctyl-9*H*-fluorene in excess carbazole under

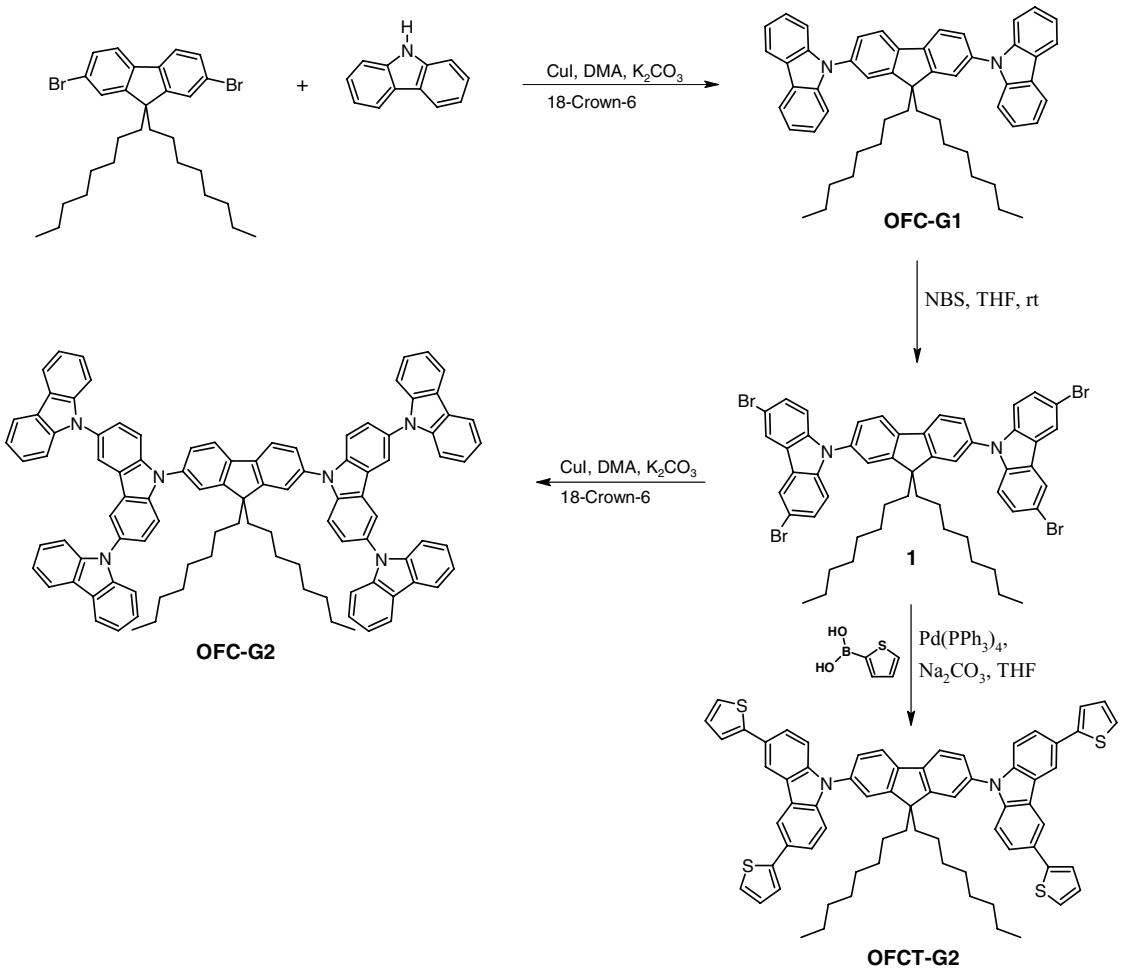

Scheme 1. Synthesis of **OFC-G1**, **OFC-G2** and **OFCT-G2**.

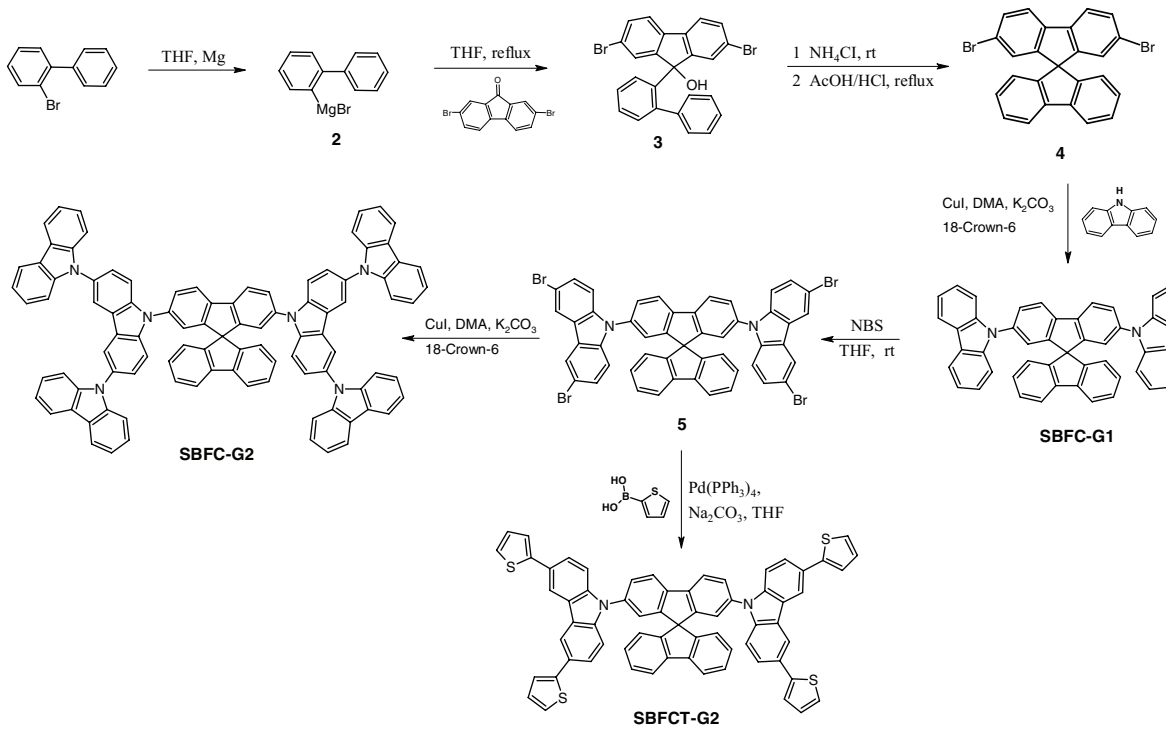

Scheme 2. Synthesis of **SBFC-G1**, **SBFC-G2** and **SBFCT-G2**.

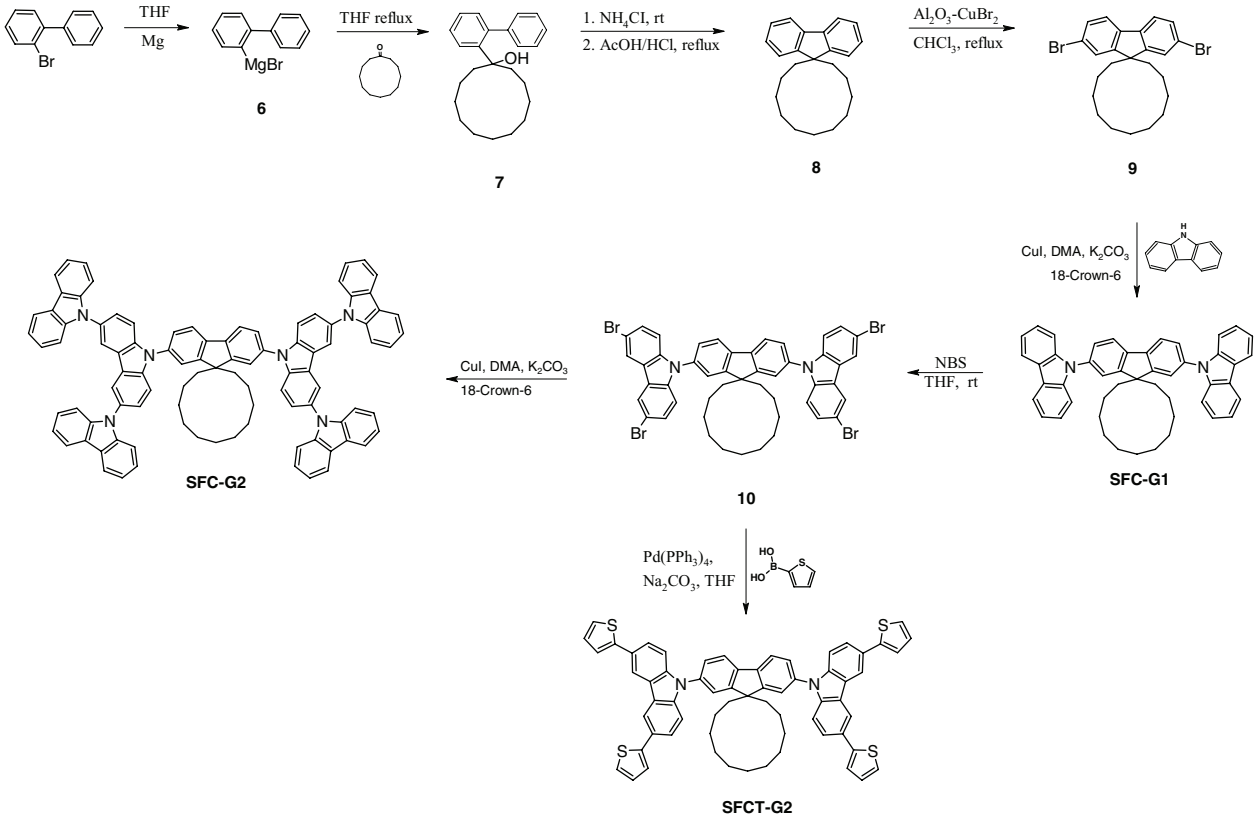

Scheme 3. Synthesis of **SFC-G1**, **SFC-G2** and **SFCT-G2**.

Ullmann coupling conditions in the presence of copper(I) iodide as catalyst and potassium carbonate as base in *N,N′*-dimethylacetamide (DMAc) at reflux temperature gave a white solid (**OFC-G1**) of 85% yield. Bromination of **OFC-G1** with *N*-bromosuccinimide (NBS) in tetrahydrofuran (THF) selectively produced the corresponding tetrabromo compound **1**, which was then reacted with carbazole under the same Ullmann coupling conditions to yield **OFC-G2**. Coupling of the intermediate **1** with an excess of 2-thiopheneboronic acid under palladium catalyzed Suzuki cross-coupling conditions gave **OFCT-G2** as a light green solid in good yield. 2,7 Dibromo-9,9′-spirobifluorene and 2,7-bis(carbazol-9-yl)-9,9′-spiro(cyclododecane-1,9′-fluorene) were prepared according to procedures previously described in literatures.[20,21] First and second generation carbazole dendrimers (**SBFC-G1**, **SFC-G1**, **SBFC-G2**, **SFC-G2**) with spirobi(fluorene) and spiro(cyclododecane-fluorene) core unit synthesized under Ullmann coupling conditions were obtained as white solids in good yields. Compound **SBFCT-G2** and **SFCT-G2** were synthesized under Suzuki cross-coupling conditions and were obtained as light green and white solids, respectively.

All the synthesized compounds were characterized by ^{1}H NMR, ^{13}C NMR, FTIR spectroscopy and MALDI-TOF. The data were found to be in good agreement with the proposed structures. All dendrimers were highly soluble in organic solvents such as chloroform, chlorobenzene, toluene and THF at room temperature. Transparent and stable amorphous films of these dendrimers can be prepared by spin-coating from solutions.

2.2. Thermal Properties

The thermal properties of the compounds were determined by DSC and TGA under nitrogen atmosphere with a heating rate of 10 °C min^{-1}. DSC was performed in the temperature range between 30 and 270 °C. TGA data revealed that all the dendrimers are thermally stable materials as summarized in **Table 1**. Their thermal decomposition temperatures (T_d) are in the range of 488–650 °C and are increased with increasing the number of carbazole moieties in the periphery. Except for **OFC-G1**, T_g values of the compounds are higher than those of commercially available TPD (T_g ~ 65 °C) and NPB (T_g ~ 100 °C) and it varies depending upon the number of carbazole and thiophene moieties, rigid octylfluorene, spirobi(fluorene) and spiro(cylododecane-fluorene) core and their structural symmetry.[9,22] There is no observed exothermic peak resulting from the crystallization of **SBFC-G2** and **SFC-G2** up to 270 °C in their DSC curves. These results indicate that they have excellent amorphous glass state stability.[23] As shown in Table 1, second generation carbazole dendrimers containing spirobi(fluorene) and spiro(cylododecane-fluorene) cores have higher values of T_d and T_g relative to their analogs.

2.3. Optical Properties

The compounds absorb in the UV spectral region below 400 nm with maxima between 320 and 350 nm. The absorption spectra are thus not significantly shifted in comparison to the spectrum of the carbazole subchromophore (*N*-phenyl carbazole, λ_a^{max} = 340 nm). The chromophore system does not extend over the whole molecule due to torsion between the carbazole and fluorene subchromophores. The torsion of the subchromophores around the σ-bonding in the ground state is also visible through the long tail of the long wavelength absorption edge. A comparison of the spectra with the molecular structures shows that compounds with the same carbazole units exhibit almost identical spectral features. Obviously, the absorption is basically determined by the carbazole unit and the attached substituents. Based on the carbazole structure one can differentiate three types spectral features. i) Unsubstituted carbazoles (**OFC-G1**, **SBFC-G1**, **SFC-G1**): $\lambda_a^{max} \approx$ 340 nm, $\varepsilon \approx$ 35000 M^{-1}cm^{-1}, ii) carbazole dendrimers (**OFC-G2**, **SBFC-G2**, **SFC-G2**): $\lambda_a^{max} \approx$ 340 nm, $\varepsilon \approx$ 60000 M^{-1}cm^{-1}. The spectral shapes of (i) and (ii) are nearly the same, except the absorption at 294 nm. The peaks at 294 nm are due to local transitions in the carbazole subchromophore (carbazole in cyclohexane: λ_a = 291 nm, $\varepsilon \approx$ 24000 M^{-1}cm^{-1}). iii) (**OFCT-G2**, **SBFCT-G2**,

Table 1. Physical and photophysical data of dendrimeric HTLs.

Compound	T_g [a] [°C]	T_d [b] [°C]	λ_{abs} [c] [nm]	λ_{em} [c] [nm]	Φ_F [c]	τ_F [c] [ns]	E_g [d] [eV]	E_{onset} [e] [eV]	HOMO/LUMO [f] [eV]	$E_{1/2}$ [h] [eV]	HOMO/LUMO [i] [eV]
OFC-G1	64	488	341	363	0.37	0.67	3.40	1.18	–5.57/–2.17 [g]	1.27	–5.66/–2.26 [j]
SBFC-G1	174	587	344	367	0.50	0.75	3.36	1.20	–5.59/–2.23 [g]	1.28	–5.67/–2.31 [j]
SFC-G1	166	552	333/340	363	0.30	0.74	3.43	1.20	–5.59/–2.16 [g]	1.28	–5.67/–2.24 [j]
OFC-G2	253	505	342	388	0.35	2.0	3.24	0.99	–5.38/–2.14 [g]	1.16	–5.55/–2.31 [j]
SBFC-G2	–	650	343	387	0.11	1.91	3.24	1.06	–5.45/–2.21 [g]	1.18	–5.57/–2.33 [j]
SFC-G2	–	629	341	389	0.09	1.96	3.24	1.07	–5.46/–2.22 [g]	1.23	–5.62/–2.38 [j]
OFCT-G2	186	500	319/340	387/406	0.05	1.08	3.18	1.00	–5.39/–2.21[g]	1.04	–5.43/–2.25 [j]
SBFCT-G2	227	617	318/341	388	0.11	1.04	3.18	0.97	–5.36/–2.18 [g]	1.01	–5.40/–2.22 [j]
SFCT-G2	205	586	318/336	388/409	0.04	1.03	3.18	0.98	–5.37/–2.19 [g]	1.03	–5.42/–2.24 [j]

[a] Obtained from DSC measurements. [b] Obtained from TGA measurements. [c] Solvent $CHCl_3$, In case of structured spectra the maxima are underlined. [d] Optical band gap. [e] Onset potentials. [f] HOMO/LUMO energy levels was calculated with reference to ferrocene (4.8 eV) according to onset potentials. [g] LUMO energy level was derived from the relation, E_g = HOMO–LUMO (where the band gap was derived from the observed optical edge). [h] Half-wave potentials. [i] HOMO/LUMO energy levels was calculated with reference to ferrocene (4.8 eV) according to half-wave potentials.

SFCT-G2): Thiophene substitution causes a redshift of the long wavelength absorption edge with an additional absorption transition appearing as a shoulder around 375 nm as well as an hyperchromic band at 320 nm with $\varepsilon \approx 80000\ M^{-1}cm^{-1}$.

The peak at 308 nm is observed only for spirobifluorenyl compounds. The 9,9′-substitution on fluorene has insignificant influence on the spectral shape, however on the position of the long wavelength absorption edge. Independent from the carbazole unit the redshift of the absorption edge increases in the order of spirocyclododecanyl, dioctyl, and spirobifluorenyl. The decrease of steric hindrance follows the same order.

The compounds fluoresce in the spectral region between 350 and 450 nm with fluorescence quantum yields between 5% and 50%. Measurements of the fluorescence and fluorescence excitation spectra at different excitation and emission wavelength as well as the comparison of the fluorescence excitation and the absorption spectra confirm the purity of the studied compounds. Spectra, quantum yields and fluorescence lifetimes of the unsubstituted fluorene-carbazole compounds (**OFC-G1**, **SBFC-G1**, **SFC-G1**: $\Phi_f \approx 0.4$, $\tau \approx 0.7$ ns) are similar. Carbazole dendrimers and thiophene substituted carbazole dendrimers show a red shift of the spectra with similar band shapes. Within each group no significant differences of the lifetimes are observed (**OFC-G2**, **SBFC-G2**, **SFC-G2**: $\tau \approx 2$ ns; **OFCT-G2**, **SBFCT-G2**, **SFCT-G2**: $\tau \approx 1$ ns). However, clear differences can be seen in the fluorescence quantum yield (Table 1).

2.4. Electrochemical Properties

The electrochemical properties of all compounds were investigated by cyclic voltammetry and the resulting data are summarized in Table 1. CV experiment was carried out in degassed anhydrous acetonitrile-dichloromethane (2:1, v:v) solutions. HOMO and LUMO energy levels of dendrimers were calculated according to the inner reference ferrocene redox couple $E°(Fc/Fc^+) = +0.41$ V vs. Ag/AgCl in acetonitrile by using the formula $E_{HOMO} = -e(E_{ox}-E_{Fc}) + 4.8$.[24] Even though determination of optical as well as electrochemical band gap from peak values rather than the ill-defined onset values is argued to have a strong theoretical basis the approach that is widely used by many authors is to use onset values. On the other hand, half-wave potential values are also used for this calculation. Because of these approaches, onset or half-wave oxidation potential values were taken into account while calculating HOMO energy levels and they were found to be between –5.36 and –5.59 eV; –5.40 and –5.67 eV according to onset and half-wave potential values, respectively. Besides, LUMO energy levels were calculated by subtracting the optical band gap from HOMO levels (Table 1). These results suggest that oxidation potentials of second generation dendrimers are lower than that of the first generation and thiophene moieties in the periphery decrease the oxidation potentials.

2.5. Electroluminescent Properties

In order to investigate the effect of hole-transporting properties of the synthesized compounds embedded between PEDOT:PSS and emitting layer (Alq_3), OLED devices were fabricated with

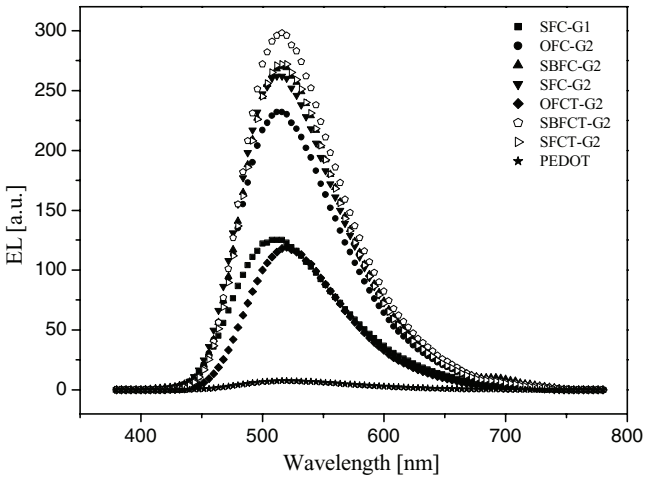

Figure 2. EL spectrum of the ITO/PEDOT:PSS/Dendrimer/Alq_3/LiF:Al OLED devices.

a configuration of ITO/PEDOT:PSS/HTL/Alq_3/LiF:Al where **SFC-G1**, **OFC-G2**, **SBFC-G2**, **SFC-G2**, **OFCT-G2**, **SBFCT-G2** and **SFCT-G2** were used as HTL materials, Alq_3 as a light emitting and ETL material, ITO and LiF:Al as anode and cathode, respectively. The reference device based on ITO/PEDOT:PSS/Alq_3/LiF:Al was fabricated to evaluate the effect of the interfacial layer in the hole injection properties.

EL spectra of all devices are shown in **Figure 2**. They emitted bright green luminescence (λ_{max} = 512–520 nm) in agreement with the PL spectrum of Alq_3. Since the HTL materials reported in this paper are dendrimers (i.e,. nonplanar molecular structure), no emissions at the longer wavelength from the exciplex species were observed from their OLED devices. Figure 2 clearly shows that, in all devices, charge recombinations occurred in Alq_3 layer. Such an interference is usually occurred in the devices fabricated from planar molecules used as HTL materials due to the exciplex formation at the interface of HTL and ETL materials.[8] In our case, the formation of exciplex is prevented by the dendronic bulky groups of both carbazoles and thiophenes at the periphery of the molecules. Furthermore, the presence of longer wavelength emission from exciplex species also suggests that all the dendrimers are hole-only-materials and electron-hole recombinations occurs only in the emitting layer (Alq_3). From HOMO-LUMO energies of the materials, the barrier for electron-migration at the interface of Alq_3/dendrimers is about 30% higher than that for hole-migration at dendrimers/Alq_3 (Table 1, **Figure 3**). Thus, from the present device configuration, while the dendrimers are acting as hole transporting materials, Alq_3 is preferably behaving as an electron blocker more than as a hole blocker; and then the charges efficiently recombine in the emitting layer.

Figure 4 shows the current-voltage and luminance-voltage characteristics of the devices containing the dendrimers as HTLs and reference device as well. The electrical parameters obtained from OLED devices with different dendrimeric HTLs are summarized in **Table 2**. From their luminance-voltage characteristics (Figure 4a), OLED devices based on **SBFCT-G2** and **SFCT-G2** exhibit the lowest turn-on voltages to obtain

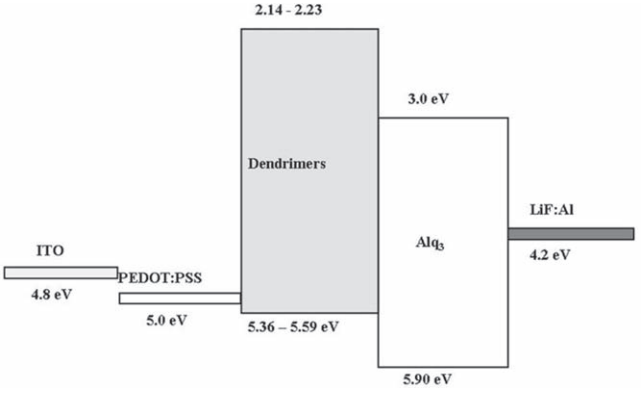

Figure 3. Energy band diagram of ITO/PEDOT:PSS/Dendrimer/Alq_3/LiF:Al devices.

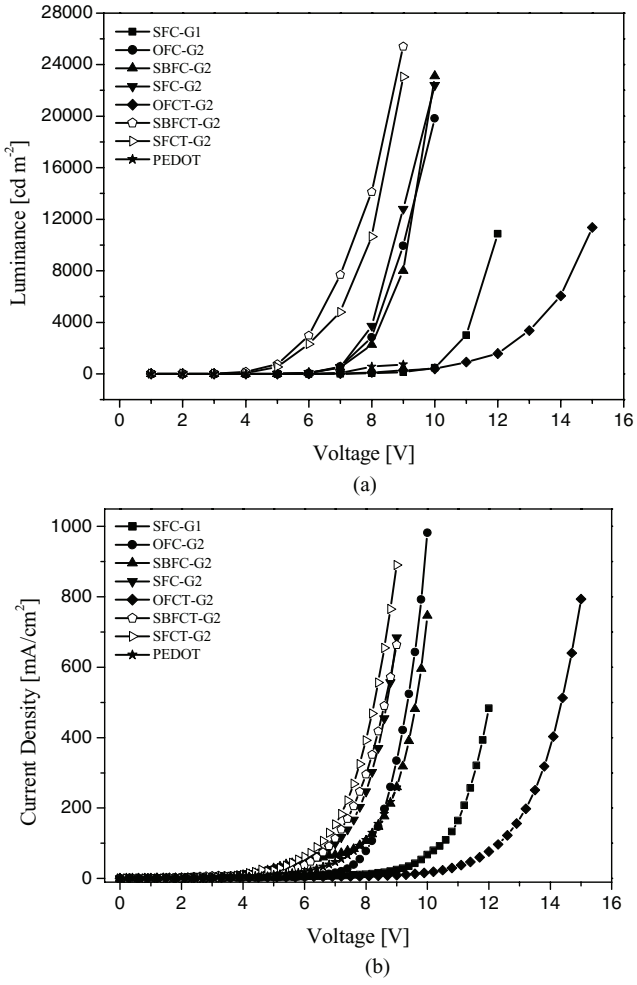

Figure 4. a) Luminescence-applied voltage characteristics and b) current density-applied voltage characteristics of the ITO/PEDOT:PSS/Dendrimer/Alq_3/LiF:Al devices.

the luminance of 1 cd m^{-2} at 2.5 and 3 V, respectively. From Figure 4a, it is very clear that the brightness observed in all devices containing synthesized HTLs is much larger through the whole voltage range when it is compared to that of reference device. Maximum luminances of 25400 and 23000 cd m^{-2} were achieved at 9 V by incorporating of **SBFCT-G2** and **SFCT-G2**, respectively. From the current-voltage characteristics as depicted in Figure 4b, the current density of devices with interfacial layers is larger than reference device with exception of **SFC-G1** and **OFCT-G2** giving lower current density at higher driving voltages. HOMO level of **SFC-G1** does not give a significant improvement of hole injection in comparison of other devices with dendrimers because of mismatch of energy level profile between PEDOT:PSS and light emitting layers. As a consequence, the height of interfacial barrier for hole injection from PEDOT:PSS to HTLs and bulk transport properties play an important role on the increase in the current density and the decrease in the operating voltage. Low current density of device containing **OFCT-G2** is thought to be the poorest hole transport property because of linear alkyl chains at fluorene core.

Figure 5 shows luminous efficiency-current density characteristics of fabricated devices. According to this figure, all dendrimers improved the luminance and current efficiency of standard ITO/PEDOT:PSS/Alq_3/LiF:Al device. Maximum luminous efficiency of 7.7 cd A^{-1} was achieved at 38 mA cm^{-2} by incorporating **SBFCT-G2**. The devices based on spiro functionalized cores containing thiophene units at their peripheral carbazole dendrons (**SBFCT-G2** and **SFCT-G2**) as HTLs have much better performance in terms of brightness, current density and current efficiency than the others. While

Table 2. The electrical parameters of OLED devices with and without dendrimeric HTLs.

Device	Turn-on voltage [V]	λ_{EL} [nm]	Maximum luminance [cd m^{-2}]	CIE_X	CIE_Y	Maximum EL efficiency [cd A^{-1}]
ITO/PEDOT:PSS/SFC-G1/Alq_3/LiF:Al	6	512	10800	0.27	0.49	2.2
ITO/PEDOT:PSS/OFC-G2/Alq_3/LiF:Al	4	516	19800	0.28	0.52	3.6
ITO/PEDOT:PSS/SBFC-G2/Alq_3/LiF:Al	3	516	23100	0.28	0.53	3.1
ITO/PEDOT:PSS/SFC-G2/Alq_3/LiF:Al	2.5	512	22400	0.28	0.52	1.9
ITO/PEDOT:PSS/OFCT-G2/Alq_3/LiF:Al	5	520	11300	0.29	0.55	2.8
ITO/PEDOT:PSS/SBFCT-G2/Alq_3/LiF:Al	2.5	516	25400	0.28	0.53	7.7
ITO/PEDOT:PSS/SFCT-G2/Alq_3/LiF:Al	3	516	23000	0.28	0.54	3.7
ITO/PEDOT:PSS/Alq_3/LiF:Al	5	520	700	0.31	0.51	0.5
ITO/PEDOT:PSS/TPD/Alq_3/LiF:Al [25]	3	520	1760	–	–	8.2

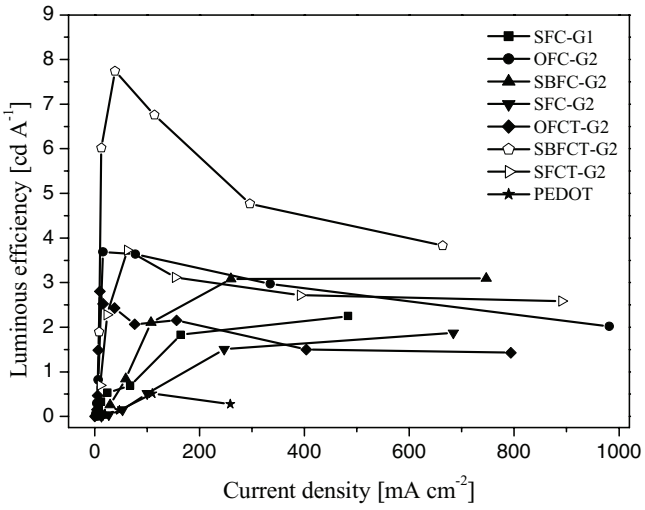

Figure 5. The luminous efficiency-current density characteristics of the ITO/PEDOT:PSS/Dendrimer/Alq_3/LiF:Al devices.

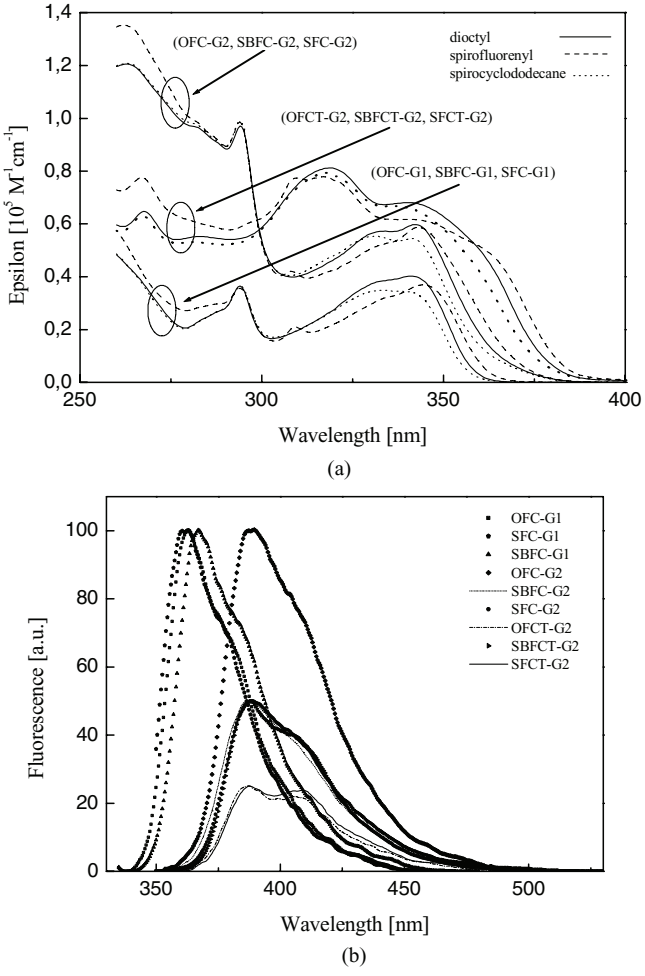

Figure 6. a) Absorption and b) fluorescence spectra in chloroform at room temperature.

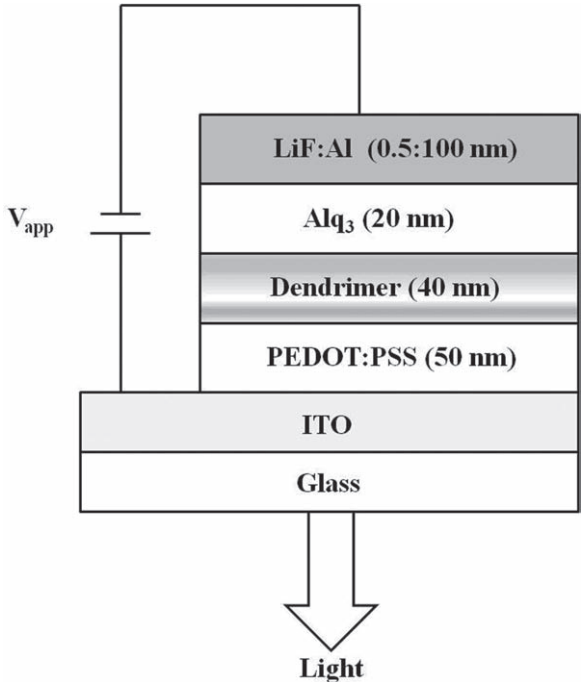

Figure 7. General device structure (ITO/PEDOT:PSS/Dendrimer/Alq_3/LiF:Al) of OLEDs and chemical structure of Alq_3.

dendrimeric HTLs whose peripheral carbazoles endcapped by thiophenes act as a superior HTL material, those endcapped by carbazoles (**SBFC-G2** and **SFC-G2**) do not show such a good performance. The current densities of OLEDs fabricated from synthesized dendrimeric HTLs were increased by endcapping with thiophene in comparison to other devices. The higher current densities and luminance values at low driving voltages of OLED fabricated from **SBFCT-G2** compared to other molecules can be attributed to well interfacial matching due to HOMO level alignment between PEDOT:PSS and Alq_3 via endcapping with thiophenes instead of bare fluorene-carbazole molecules (**OFC-G2**, **SBFC-G2**, **SFC-G2** and **SFC-G1**). These results show that substitution of core molecules by donor moieties like thiophene can increase HOMO level of the whole molecule. As a result, this HOMO level shift leads to a decrease in the height of interfacial barrier of HTLs, and then hole injection from PEDOT:PSS to HTL can occur efficiently.

Mu et al. investigated the performance of OLED device with Alq_3/TPD active regions using various anode and cathode electrode structures.[25] They achieved the best performance from an OLED device with a configuration of ITO/PEDOT:PSS(50 nm)/TPD(50 nm)/Alq_3(40 nm)/LiF:Al(1:100 nm). The electrical parameters obtained from this OLED device are summarized in Table 2. They reported maximum luminance of 1720 cd m^{-2} at 25 V, a turn-on voltage of 3 V and EL efficiency of 8.2 cd A^{-1} at a brightness of 100 cd m^{-2} and 5 V. When the results published by Mu et al. are compared with this present study, fluorene-carbazole dendrimers reported here have better hole transporting ability than commonly used HTM of TPD.

3. Conclusion

Novel hole transporting dendrimers were synthesized by divergent synthesis method. The measurements of ^{1}H NMR, ^{13}C NMR, FTIR, and MALDI-TOF are in agreement with the chemical structures expected. CV, TGA and DSC results indicate that except for **OFC-G1** all compounds are electrochemically and thermally stable amorphous materials. Second generation carbazole dendrimers with spirobi(fluorene) and spiro(cylododecane-fluorene) core unit (**SBFC-G2** and **SFC-G2**) have higher values of T_d and T_g than the others (Table 1). This indicates that the increasing of generation number, rigid core unit and carbazole groups increase the T_d and T_g values of dendrimers. The mutilayer OLED device containing **SFCT-G2** as HTL material showed maximum performance and exhibited bright green emission with a peak centered at 516 nm and CIE coordinates of (0.28, 0.54). The maximum luminance and luminous efficiency of this device were obtained as 25400 cd m^{-2} and 7.7 cd A^{-1}, respectively. The dendrimers containing electron donating thiophene groups in the periphery are more favorable to be used as HTL material in OLEDs because of good energy level alignment between HOMO levels of PEDOT:PSS and the emissive layer.

4. Experimental Section

All reagents and solvents were purchased from Aldrich and used without further purification. Alq_3 and PEDOT:PSS for EL device fabrication were also obtained from Aldrich and H. C. Starck, respectively.

Absorption spectra were recorded on a LAMBDA 16 spectrophotometer (Perkin Elmer). Fluorescence emission and excitation spectra were measured using a LS50B luminescence spectrometer (Perkin Elmer). Fluorescence quantum yields were calculated relative to quinine sulphate (purum; FLUKA) in 0.1 N H_2SO_4 (pro analysi; Laborchemie Apolda) used as a standard ($\Phi_f = 0.55$). The absorbance at the excitation wavelength was kept below 0.05 for the samples and the reference.

The kinetics of fluorescence was investigated with a CD900 time correlating single photon counting spectrometer (Edinburgh Instruments). The excitation source was a hydrogen filled nanosecond flash lamp which yielded an instrument response pulse of 1.3 ns FWHM. Polarizers (magic angle) were used to avoid polarization effects. The kinetics of fluorescence was recorded at the emission maxima under excitation at the longest wavelength absorption maxima. The spectral slit width was 18 nm. Decay curves were accumulated until 5000 counts in the maximum with at least 10^3 occupied channels. The channel width corresponded to 13 ps. In order to calculate the fluorescence lifetime, the software package implemented in the Edinburgh Instruments software was used. (The analysis makes use of the iterative reconvolution technique and the Marquardt fitting algorithm.) Plots of weighted residuals and of the autocorrelation function and values of reduced residuals $\chi 2$ were used to judge the quality of the fit. $\chi 2$ values larger than 1.3 were not accepted.

2,7-Dibromo-9,9′-spirobifluorene,[20] 2,7-bis(carbazol-9-yl)-9,9′-spiro(cyclododecane-1,9′-fluorene)[21] were synthesized following the procedures published in the literature. ^{1}H and ^{13}C NMR spectra were recorded with a Bruker 400 MHz spectrometer with chloroform-d as the solvent if otherwise not stated and tetramethylsilane as the internal standard. FTIR spectra were recorded by a Perkin Elmer FTIR Spectrum One by using ATR system (4000–650 cm^{-1}). DSC and TGA measurements were performed under a nitrogen atmosphere with a heating rate of 10 °C min^{-1} on Perkin Elmer Pyris 6 DSC and Perkin Elmer Pyris 6 TGA, respectively. Electrochemical measurements were performed using a CHI660B electrochemical workstation from CH Instruments (Austin, TX, USA). A conventional three-electrode configuration in 0.1 M solution of tetrabutylammonium hexafluorophosphate dissolved in acetonitrile:dichloromethane (2:1; v:v) with a scan rate of 100 mV s^{-1} with a platinum working electrode, a Pt-wire counter electrode, and an Ag/AgCl reference electrode was used. MALDI-TOF spectrum was recorded by using Applied Biosystems Voyager System 6020.

Indium tin oxide (ITO) glass substrate with a sheet resistance of 15Ω □$^{-1}$ was used. After etching and cleaning the ITO-glass substrates in ultrasonic bath with acetone and *iso*-propanol according to standard cleaning procedure, an active area of 10 mm^2 was obtained. PEDOT:PSS was spin coated onto the substrate at a spin speed of 4000 rpm for 30 s forming 50 nm thick layer. The samples were annealed under nitrogen atmosphere for 30 min at 150 °C. Chlorobenzene solutions of dendrimers (1.5%, w/v) were spin-coated onto ITO-glass substrates at a spin speed of 3000 rpm for 30 s to get a 40 nm thick of HTL. Then Alq_3 as emissive layer and ETL was deposited onto the surface of the dendrimers' films with a thickness of 20 nm. Finally, an ultra thin layer of LiF (0.5 nm) and Al cathode (100 nm) were evaporated under high vacuum by employing shadow mask. The characterization of fabricated devices was carried out under inert nitrogen environment inside a glove box system. A Keithley 236 source meter was used to investigate I–V characteristics. The EL and luminance properties were measured using Spectrascan PR-655 spectroradiometer. The thicknesses of films were determined with a Digital Instrument 3100 atomic force microscope (AFM).

Synthesis of 2,7-bis(carbazol-9-yl)-9,9-bis-n-octylfluorene (**OFC-G1**): opper(I) iodide (0.028 g, 0.15 mmol), 18-crown-6 (0.013 g, 0.05 mmol), potassium carbonate (0.825 g, 6 mmol), carbazole (1 g, 6 mmol), and DMAc (7.5 mL) were added to a round-bottom flask and vigorously stirred at 165 °C under argon. After stirring and refluxing for 2 h, 2,7-dibromo-9,9-dioctyl-9*H*-fluorene (1.64 g, 3 mmol) as a solution in hot DMAc (7.5 mL) was added into the mixture slowly. The final reaction medium was heated to reflux for 24 h. The reaction solution was poured into water (300 mL), the precipitate was collected by filtration, dried and purified by column chromatography over silica gel eluting with a mixture of dichloromethane:*n*-hexane (1:4) followed by recrystallization from a mixture of dichloromethane-methanol gave a white solid (1.83 g, 85%). ^{1}H NMR (400 MHz, $CDCl_3$, 25°C, TMS): δ (ppm) = 8.22–8.20 (d, 4H), 8.01–7.99 (d, 2H), 7.63–7.61 (d, 4H), 7.50–7.45 (m, 28H), 7.36–7.32 (m, 4H), 2.09–2.04 (m, 4H), 1.17 (broad s, 18H), 0.91–0.89 (m, 6H); ^{13}C NMR (100 MHz, $CDCl_3$, 25°C, TMS): δ (ppm) = 153.3, 141.5, 140.0, 137.2, 126.4, 123.9, 122.3, 121.4, 120.9, 120.4, 110.2, 56.1, 40.6, 32.2, 30.4, 29.8, 29.7, 24.6, 23.0, 14.5; IR (ATR): ν = 3061, 2921, 2846, 2657, 2323, 2107, 1594, 1467, 1443, 1330, 1309, 1225, 819, 744, 715 cm^{-1}; MALDI-TOF (m/z): [M^+] calcd. for $C_{53}H_{56}N_2$, 721.0252; found 720.3300.

Synthesis of 9,9′-(9,9-dioctyl-9H-fluorene-2,7-diyl)bis(3,6-dibromo-9H-carbazole) (**1**): NBS (1.41 g, 8 mmol) was added in small portions to a solution of **OFC-G1** (1.44 g, 2 mmol) in THF (50 mL). The reaction mixture was stirred at room temperature under argon atmosphere for 18 h. THF was removed to dryness and dichloromethane (100 mL) was added to the resulting solid. The organic phase was washed with water (2×100 mL), brine (100 mL), dried over anhydrous Na_2SO_4, filtered and the solvent was removed under vacuum. Purification by recrystallization from a mixture of dichloromethane-methanol gave a white solid (1.86 g, 90%). ^{1}H NMR (400 MHz, $CDCl_3$, 25°C, TMS): δ (ppm) = 8.12 (d, 4H), 7.9–7.88 (d, 2H), 7.45–7.42 (d, 8H), 7.21–7.19 (d, 4H), 1.97–1.93 (m, 4H), 1.05 (broad s, 21H), 0.75–0.71 (m, 9H); IR (ATR): 2921, 2846, 2323, 2107, 1607, 1465, 1432, 1360, 1279, 1231, 1056, 1018, 860, 798, 634 cm^{-1}.

Synthesis of 9′,9″-(9,9-dioctyl-9H-fluorene-2,7-diyl)bis-9′H-9,3′:6′,9″-tercarbazole (**OFC-G2**): Copper(I) iodide (0.014 g, 0.075 mmol), 18-crown-6 (0.0065 g, 0.0025 mmol), potassium carbonate (0.412 g, 3 mmol), carbazole (0.5 g, 3 mmol), and DMAc (4 mL) were added to a round-bottom flask and vigorously stirred at 165 °C under argon. After stirring and refluxing for 2 h, **1** (0.77 g, 0.75 mmol) as a solution in hot DMAc (4 mL) was added into the mixture slowly. The final reaction medium was heated to reflux for 24 h. The reaction solution was poured into water (150 mL), the precipitate was collected by

filtration, dried and purified by column chromatography over silica gel eluting with a mixture of dichloromethane:*n*-hexane (1:2) followed by recrystallization from a mixture of dichloromethane-methanol gave white solid (0.82 g, 80%). ^{1}H NMR (400 MHz, $CDCl_3$, 25°C, TMS): δ (ppm) = 8.33 (d, 4H), 8.18–8.16 (d, 10H), 7.81–7.79 (m, 4H), 7.74–7.71 (m, 4H), 7.68–7.65 (dd, 4H), 7.42–7.41 (t, 4H), 7.31–7.28 (m, 8H), 2.23–2.19 (m, 4H), 1.19–1.14 (m, 21H), 1.00–0.97 (m, 4H), 0.73–0.69 (m, 5H); ^{13}C NMR (100 MHz, $CDCl_3$, 25°C, TMS): δ (ppm) = 142.0, 141.0, 130.7, 126.6, 126.1, 124.3, 123.4, 120.6, 120.0, 109.9, 32.02, 29.6, 29.4, 22.8, 14.2; IR (ATR): ν = 3045, 2916, 2846, 2663, 2318, 2102, 1588, 1465, 1448, 1333, 1314, 1276, 1225, 1016, 801, 741, 717, 634 cm^{-1}; MALDI-TOF (m/z): [M^+] calcd. for $C_{101}H_{84}N_6$, 1381.7881; found 1381.6800.

Synthesis of 9,9′-(9,9-dioctyl-9H-fluorene-2,7-diyl)bis(3,6-di-2-thienyl-9H-carbazole) (**OFCT-G2**): A mixture of **1** (0.77 g, 0.75 mmol), 2-thiopheneboronic acid (0.38 g, 3 mmol), $Pd(PPh_3)_4$ (0.02 g, 0.02 mmol), aqueous solution of 2 M Na_2CO_3 (12.5 mL, 25.00 mmol) and THF (20 mL) was degassed with Ar for 5 minute. The reaction mixture was stirred at reflux under Ar for 24 h. After being cooled to room temperature, distilled water (100 mL) was added. The mixture was extracted with dichloromethane (2 × 50 mL), washed with water (100 mL) and brine (100 mL), dried over anhydrous Na_2SO_4, filtered and the solvents were removed under vacuum. Purification by column chromatography over silica gel eluting with a mixture of dichloromethane:*n*-hexane (1:2) afforded pale green solids (0.67 g, 85%). ^{1}H NMR (400 MHz, $CDCl_3$, 25°C, TMS): δ (ppm) = 8.44 (d, 4H), 8.03–8.01 (d, 2H), 7.75–7.72 (dd, 4H), 7.64–7.61 (d, 4H), 7.48–7.46 (d, 4H), 7.41–7.40 (dd, 4H), 7.31–7.30 (dd, 4H), 7.16–7.13 (m, 4H), 2.08–2.06 (m, 3H), 1.20 (broad s, 27H), 0.85–0.82 (t, 4H); ^{13}C NMR (100 MHz, $CDCl_3$, 25°C, TMS): δ (ppm) = 145.5, 141.1, 139.9, 128.2, 127.4, 125.2, 124.2, 124.1, 122.6, 110.5, 56.0, 32.1, 30.2, 29.8, 29.6, 29.5, 22.8, 14.3; IR (ATR): ν = 2916, 2846, 2657, 2345, 2102, 1913, 1604, 1580, 1475, 1427, 1357, 1284, 1225, 870, 801, 685 cm^{-1}; MALDI-TOF (m/z): [M^+]: calcd. for $C_{69}H_{64}N_2S_4$, 1049.5239; found 1048.3900.

Synthesis of 9,9′-(9,9′-spirobi[fluorene]-2,7-diyl)bis-9H-carbazole (**SBFC-G1**): Copper(I) iodide (0.028 g, 0.15 mmol), 18-crown-6 (0.013 g, 0.05 mmol), potassium carbonate (0.825 g, 6 mmol), carbazole (1 g, 6 mmol), and DMAc (7.5 mL) were added to a round-bottom flask and vigorously stirred at 165 °C under argon. After stirring and refluxing for 2 h, 2,7-dibromo-9,9′-spirobifluorene (1.42 g, 3 mmol) as a solution in hot DMAc (7.5 mL) was added into the mixture slowly. The final reaction medium was heated to reflux for 24 h. Then the reaction solution was poured into water (300 mL), the precipitate was collected by filtration, dried and purified by column chromatography over silica gel eluting with a mixture of dichloromethane:*n*-hexane (1:4) followed by recrystallization from a mixture of dichloromethane-methanol gave a white solid (1.64 g, 85%). ^{1}H NMR (400 MHz, $CDCl_3$, 25°C, TMS): δ (ppm) = 8.13–8.12 (d, 2H), 8.08–8.06 (d, 4H), 7.77–7.75 (d, 2H), 7.67–7.64 (dd, 2H), 7.39–7.37 (d, 2H), 7.35–7.34 (dd, 1H), 7.32–7.30 (d, 4H), 7.25–7.20 (m, 11H), 7.01–7.00 (d, 2H); ^{13}C NMR (100 MHz, $CDCl_3$, 25°C, TMS): δ (ppm) = 151.4, 147.8, 142.0, 140.8, 140.2, 137.6, 128.4, 126.8, 126.0, 123.9, 123.5, 123.0, 121.4, 120.5, 120.4, 120.1, 119.6, 110.7, 109.8. IR (ATR): ν = 3045, 2657, 2355, 2118, 1594, 1470, 1443, 1330, 1311, 1228, 1153, 819, 741, 717 cm^{-1}; MALDI-TOF (m/z): [M^+] calcd. for $C_{49}H_{30}N_2$, 646.776; found 646.1400.

Synthesis of 9,9′-(9,9′-spirobi[fluorene]-2,7-diyl)bis(3,6-dibromo-9H-carbazole) (**5**) NBS (1.41 g, 8 mmol) was added in small portions to a solution of **SBFC-G1** (1.29 g, 2 mmol) in THF (50 mL). The reaction mixture was stirred at room temperature under argon atmosphere for 18 h. THF were removed to dryness than dichloromethane (100 mL) was added to the resulting solid. The organic phase was washed with water (2 × 100 mL), brine (100 mL), dried over anhydrous Na_2SO_4, filtered and the solvents were removed under vacuum. Purification by recrystallization from a mixture of dichloromethane-methanol gave a white solid (1.73 g, 90%). ^{1}H NMR (400 MHz, $CDCl_3$, 25°C, TMS): δ (ppm) = 8.07–8.06 (d, 2 H), 8.01(s, 1H), 7.99 (s, 1H), 7.82–7.76 (m, 4H), 7.57–7.54 (dd, 2H), 7.49–7.47 (dd, 2H), 7.40–7.34 (m, 6H), 7.19–7.15 (t, 2H), 7.01–6.98 (d, 2H), 6.93–6.92 (d, 1H), 6.84–6.80 (t, 3H); IR (ATR): ν = 3045, 2657, 2318, 2113, 1602, 1465, 1430, 1276, 1228, 1053, 1016, 860, 803, 725, 631 cm^{-1}.

Synthesis of 9′,9″-(9,9′-spirobi[fluorene]-2,7-diyl)bis-9′H-9,3′:6′,9″-tercarbazole (**SBFC-G2**): Copper(I) iodide (0.014 g, 0.075 mmol), 18-crown-6 (0.0065 g, 0.0025 mmol), potassium carbonate (0.412 g, 3 mmol), carbazole (0.5 g, 3 mmol), and DMAc (4 mL) were added to a round-bottom flask and vigorously stirred at 165 °C under argon. After stirring and refluxing for 2 h, **5** (0.72 g, 0.75 mmol) as a solution in hot DMAc (4 mL) was added into the mixture slowly. The final reaction medium was heated to reflux for 24 h. The reaction solution was poured into water (150 mL), the precipitate was collected by filtration, dried and purified by column chromatography over silica gel eluting with a mixture of dichloromethane:*n*-hexane (1:2) followed by recrystallization from a mixture of dichloromethane-methanol gave a white solid (0.78 g, 80%). ^{1}H NMR (400 MHz, $CDCl_3$, 25°C, TMS): δ (ppm) = 8.27–8.25 (d, 2H), 8.20–8.16 (t, 11H), 7.85–7.80 (dd, 4H), 7.55–7.49 (dd, 8H), 7.41–7.33 (m, 18H), 7.31–7.25 (m, 11H), 7.20 (d, 2H), 7.10–7.08 (d, 2H); IR (ATR): ν = 3045, 2657, 2355, 2328, 2113, 1913, 1594, 1467, 1448, 1309, 1276, 1223, 1153, 809, 741, 720 cm^{-1}; MALDI-TOF (m/z): [M^+] calcd. for $C_{97}H_{58}N_6$, 1307.5389; found 1307.4600.

Synthesis of 9,9′-(9,9′-spirobi[fluorene]-2,7-diyl)bis(3,6-di-2-thienyl-9H-carbazole) (**SBFCT-G2**): A mixture of **5** (0.72 g, 0.75 mmol), 2-thiopheneboronic acid (0.38 g, 3 mmol), $Pd(PPh_3)_4$ (0.02 g, 0.02 mmol), aqueous solution of 2 M Na_2CO_3 (12.5 mL, 25.00 mmol) and THF (20 mL) was degassed with argon for 5 minute. The reaction mixture was stirred at reflux under Ar for 24 h. After being cooled to room temperature water (100 mL) was added. The mixture was extracted with dichloromethane (2 × 50 mL), washed with water (100 mL) and brine (100 mL), dried over anhydrous Na_2SO_4, filtered and the solvents were removed under vacuum. Purification by column chromatography over silica gel eluting with a mixture of dichloromethane:*n*-hexane (1:2) afforded pale green solids (0.62 g, 85%). ^{1}H NMR (400 MHz, $CDCl_3$, 25°C, TMS): δ (ppm) = 8.28 (s, 4H), 8.14–8.12 (d, 2H), 7.80–7.78 (d, 2H), 7.64–7.62 (dd, 2H), 7.57–7.55 (dd, 4H), 7.41–7.37 (t, 2H), 7.32–7.31 (d, 4H), 7.26–7.18 (m, 8H), 7.10–7.08 (t, 4H), 7.01–6.99 (d, 4H); ^{13}C NMR (100 MHz, $CDCl_3$, 25°C, TMS): δ (ppm) = 140.7, 128.2, 127.3, 124.1, 123.9, 122.5, 110.3; IR (ATR): ν = 3056, 2921, 2846, 2657, 2328, 2102, 1602, 1475, 1424, 1357, 1287, 1225, 801, 731, 682 cm^{-1}; MALDI-TOF (m/z): [M^+] calcd. for $C_{65}H_{38}N_2S_4$, 975.2747; found 974.1600.

Synthesis of 9,9′-spiro[cyclododecane-1,9′-fluorene]-2′,7′-diylbis(3,6-dibromo-9H-carbazole) (**10**): NBS (1.05 g, 6 mmol) was added in small portions to a solution of **SFC-G1** (0.97 g, 1.5 mmol) in THF (40 mL). The reaction mixture was stirred at room temperature under argon atmosphere for 18 h. THF was removed to dryness and dichloromethane (100 mL) was added to the remaning solid. The organic phase was washed with water (2 × 100 mL), brine (100 mL), dried over anhydrous Na_2SO_4, filtered and the solvents were removed to dryness. Purification by recrystallization from a mixture of dichloromethane and methanol gave a white solid (1.30 g, 90%). IR (ATR): ν = 3040, 2927, 2857, 2657, 2323, 2118, 1709, 1588, 1465, 1430, 1354, 1314, 1271, 1223, 1053, 1016, 790, 731, 631 cm^{-1}.

Synthesis of 9′,9″-spiro[cyclododecane-1,9′-fluorene]-2′,7′-diylbis-9′H-9,3′:6′,9″-tercarbazole (**SFC-G2**): Copper(I) iodide (0.009 g, 0.05 mmol), 18-crown-6 (0.004 g, 0.016 mmol), potassium carbonate (0.27 g, 2 mmol), carbazole (1 g, 2 mmol), and DMAc (2.5 mL) were added to a round-bottom flask and vigorously stirred at 165 °C under argon. After stirring and refluxing for 2 h, **10** (0.48 g, 0.5 mmol) as a solution in hot DMAc (2.5 mL) was added into the mixture slowly. The final reaction medium was refluxed for 24 h. After being cooled to room temperature, the reaction solution was poured into water (100 mL), the precipitate was collected by filtration, dried and purified by column chromatography over silica gel eluting with a mixture of dichloromethane:*n*-hexane (1:2) followed by recrystallization from a mixture of dichloromethane-methanol gave a white solid (0.52 g, 80%). ^{1}H NMR (400 MHz, $CDCl_3$, 25°C, TMS): δ (ppm) = 8.35 (s, 4H), 8.19–8.16 (t, 10H), 7.93 (s, 2H), 7.82–7.80 (d, 2H), 7.75–7.67 (dd, 8H), 7.44–7.41 (t, 16H), 7.32–7.29 (t, 8H), 2.00–1.94 (d, 7H), 1.50 (broad s, 15H); ^{13}C NMR (100 MHz, $CDCl_3$, 25°C, TMS): δ (ppm) = 142.0, 141.2, 130.7, 126.1, 124.2, 123.4, 120.5, 119.9, 119.6, 109.9; IR (ATR): ν = 3051, 2927, 2851, 2668, 2318, 2086, 1594, 1569, 1470, 1448, 1333, 1311, 1276, 1225, 1155, 1010, 919, 814,

744, 720 cm^{-1}; MALDI-TOF (m/z): [M^+] calcd. for $C_{99}H_{72}N_6$, 1309.6393; found 1309.6200.

Synthesis of 9,9′-spiro[cyclododecane-1,9′-fluorene]-2′,7′-diylbis(3,6-di-2-thienyl-9H-carbazole) (**SFCT-G2**): A mixture of **10** (0.48 g, 0.5 mmol), 2-thiopheneboronic acid (0.25 g, 2 mmol), $Pd(PPh_3)_4$ (0.013 g, 0.013 mmol), aqueous solution of 2 M Na_2CO_3 (8 cm^3, 16.00 mmol), and THF (15 mL) was degassed with Ar for 5 min. The reaction mixture was stirred at reflux under Ar for 24 h. After being cooled to room temperature water (100 mL) was added. The mixture was extracted with dichloromethane (2 × 50 mL), washed with water (100 mL) and brine (100 mL), dried over anhydrous Na_2SO_4, filtered and the solvents were removed to dryness. Purification by column chromatography over silica gel eluting with a mixture of dichloromethane:*n*-hexane (1:2) afforded white solids (0.41 g, 85%). ^{1}H NMR (400 MHz, $CDCl_3$, 25°C, TMS): δ (ppm) = 8.43 (s, 4H), 8.04–8.01 (d, 2H), 7.75–7.72 (td, 6H), 7.62–7.59 (dd, 2H), 7.47–7.44 (d, 4H), 7.40–7.39 (d, 4H), 7.30–7.28 (d, 4H), 7,14–7.12 (t, 4H); ^{13}C NMR (100 MHz, $CDCl_3$, 25°C, TMS): δ (ppm) = 155.0, 145.5, 141.3, 138.4, 136.1, 128.2, 127.3, 126.2, 125.2, 124.2, 124.0, 122.6, 121.4, 118.2, 110.5, 53.93, 23.24; IR (ATR): ν = 3061, 2927, 2851, 2652, 2355, 2323, 2118, 1604, 1580, 1475, 1424, 1360, 1284, 1228, 868, 849, 793, 739, 685; MALDI-TOF (m/z): [M^+] calcd. for $C_{64}H_{52}N_2S_4$, 977.3752; found 976.2200.

Acknowledgements

O. Usluer, S. Demic and N.S. Sariciftci thank the European Science Foundation (Research Networking Program ''New Generation of Organic based Photovoltaic Devices'' ORGANISOLAR) and the State Planning Organization of Turkey (DPT). S. Demic is also grateful to TUBITAK (project 104T191) for financial support and thanks Dr. B. F. M. de Wall and R. Bovee (Eindhoven University of Technology) for MALDI-TOFs.

Received: June 8, 2010
Published online:

[1] C. W. Tang, S. A. VanSlyke, *Appl. Phys. Lett.* **1987**, *51*, 913.
[2] S. A. Jenekhe, *Adv. Mater.* **1995**, *7*, 309.
[3] F. Hide, M. A. Diaz-Garcia, B. J. Schartz, A. J. Heeger, *Acc. Chem. Res.* **1997**, *30*, 430.
[4] J. Shinar, *Organic Light-emitting Devices*, Springer, New York, USA **2004**.
[5] P. F. Smith, P. Gerroir, S. Xie, A. M. Hor, Z. Popovic, *Langmuir* **1998**, *14*, 5946.
[6] P. Fenter, F. Schreiber, V. Bulovic, S. R. Forest, *Chem. Phys. Lett.* **1997**, *277*, 521.
[7] M. Nomura, Y. Shibasaki, M. Ueda, K. Tugita, M. Ichikawa, Y. Taniguchi, *Synth. Met.* **2005**, *148*, 155.
[8] V. Promarak, M. Ichikawa, T. Sudyoadsuk, S. Saengsuwan, S. Jungsuttiwong, T. Keawin, *Synth. Met.* **2007**, *157*, 17.
[9] Q. Zhang, J. Chen, Y. Cheng, L. Wang, D. Ma, X. Jing, F. Wang, *J. Mater. Chem.* **2004**, *14*, 895.
[10] J. Li, D. Liu, Y. Li, C.-S. Lee, H.-L. Kwong, S. Lee, *Chem. Mater.* **2005**, *17*, 1208.
[11] J. P. Chen, H. Tanabe, X.-C. Li, T. Thoms, Y. Okamura, K. Ueno, *Synth. Met.* **2003**, *132*, 173.
[12] S. Grigalevicius, L. Mab, J. V. Grazulevicius, Z.-Y. Xie, *Synth. Met.* **2006**, *156*, 46.
[13] M.-H. Ho, B. Balaganesan, T. Chu, T. Chen, C. H. Chen, *Thin Solid Films* **2008**, *517*, 943.
[14] a) F. Tran-Van, L. Beouch, F. Vidal, P. Yammine, D. Teyssiié, C. Chevrot, *Electrochim. Acta* **2008**, *53*, 4336; b) D. R. Rosseinsky, R. J. Mortimer, *Adv. Mater.* **2001**, *13*, 783; c) M. Mastragostino, in *Applications of Electroactive Polymers*, (Ed.: B. Scrosati),Chapman and Hall, London **1993**.
[15] P. M. S. Monk, R. J. Morimer, D. R. Rosseinsky, *Electrochromism: Fundamentals and Applications*, VCH, Weinheim, Germany **1995**.
[16] M. Watanabe, M. Nishiyama, T. Yamamoto, Y. Koie, *Tetrahedron Lett.* **2000**, *41*, 481.
[17] J. P. Chen, A. Natansohn, *Macromolecules* **1999**, *32*, 3171.
[18] J. Qu, R. Kawasaki, M. Shiotsuki, F. Sonda, T. Masuda, *Polymer* **2006**, *47*, 6551.
[19] a) K. S. Kim, Y. M. Jeon, J. W. Kim, C. W. Lee, M. S. Gong, *Org. Electron.* **2008**, *9*, 797; b) A. Farcas, N. Jarroux, V. Harabagiu, P. Guégan, *Eur. Polym. J.* **2009**, *45*, 795.
[20] J. Pei, J. Ni, X. H. Zhou, X. Y. Cao, *J. Org. Chem.* **2002**, *67*, 4924.
[21] O. Usluer, S. Koyuncu, S. Demic, R. A. J. Janssen, unpublished.
[22] C.-H. Chen, W.-J. Shen, K. Jakka, C.-F. Shu, *Synt. Met.* **2004**, *143*, 215.
[23] B. E. Koene, D. E. Loy, M. E. Thompson, *Chem. Mater.* **1998**, *10*, 2235.
[24] a) G. Yu, Y. Yang, Y. Cao, Q. Pei, C. Zhang, A. J. Heeger, *Chem. Phys. Lett.* **1996**, *259*, 465; b) S. Admassie, O. Inganas, W. Mammo, E. Perzon, M. R. Andersson, *Synt. Met.* **2006**, *156*, 614; c) A. Berlin, G. Zotti, S. Zecchin, G. Schiavon, B. Vercelli, A. Zanelli, *Chem. Mater.* **2004**, *16*, 3667.
[25] H. Mu, W. Li, R. Jones, A. Steckl, D. Klotzkin, *J. Lumin.* **2007**, *126*, 225.